ELSEVIER

Journal of Molecular Catalysis B: Enzymatic 15 (2001) 123–133

JOURNAL OF MOLECULAR CATALYSIS B: ENZYMATIC

www.elsevier.com/locate/molcatb

Modification of the fatty acid specificity of cytochrome P450 BM-3 from *Bacillus megaterium* by directed evolution: a validated assay

Oliver Lentz [a], Qing-Shang Li [a], Ulrich Schwaneberg [a], Sabine Lutz-Wahl [a], Peter Fischer [b], Rolf D. Schmid [a,*]

[a] *Institut für Technische Biochemie, Universität Stuttgart, Allmandring 31, D-70569 Stuttgart, Germany*
[b] *Institut für Organische Chemie, Universität Stuttgart, Pfaffenwaldring 55, D 70569 Stuttgart, Germany*

Abstract

Cytochrome P450 BM-3 (CYP102) catalyzes the subterminal hydroxylation of fatty acids with a chain length of 12–22 carbons. The paper focuses on the regioselectivity and substrate specificity of the purified wild-type enzyme and five mutated variants towards caprylic, capric, and lauric acid. The enzymes were obtained by random mutagenic fine-tuning of the mutant F87A(LARV). F87A(LARV) was selected as the best enzyme variant in a previous study in which the single mutant F87A was subjected to rational evolution to achieve hydroxylation activity for short chain length substrates using a *p*-nitrophenolate-based spectrophotometric assay.

The best mutants, F87V(LAR) and F87V(LARV), show a higher catalytic activity towards ω-(*p*-nitrophenoxy)decanoic acid (10-*p*-NCA) than F87A(LARV). In addition, they proved capable of hydroxylating ω-(*p*-nitrophenoxy)octanoic acid (8-*p*-NCA) which the wild-type enzyme is unable to do. Both variants catalyzed hydroxylation of capric acid, which is not a substrate for the wild-type, with a conversion rate of up to 57%. The chain length specificity of the mutants in fatty acid hydroxylation processes shows a good correlation with their activity towards *p*-NCA pseudosubstrates. The *p*-NCA assay therefore, allows high-throughput screening of large mutant libraries for the identification of enzyme variants with the desired catalytic activity towards fatty acids as the natural substrates.

Keywords: Cytochrome P450 CYP102; *Bacillus megaterium*; Fatty acid hydroxylation; Colorimetric assay system; High-throughput screening; Directed evolution

1. Introduction

P450 BM-3 (CYP102), a water-soluble heme enzyme (M_r 120 kDa) from *Bacillus megaterium* [1], contains an FAD- and FMN-dependent reductase domain within the same polypeptide chain. Thus, it can be regarded as self-sufficient in terms of the electron transfer from NADPH to the heme iron. While the structure of the enzyme has been resolved at 2.03 Å resolution [2], no crystallographic information exists on the functional enzyme-substrate or enzyme-inhibitor complexes. The native enzyme catalyzes the subterminal hydroxylation of fatty acids with a chain length of C_{12} to C_{22} preferentially in the (ω-1/2/3) positions and with high enantioselectivity in the ω-1 and ω-2 positions (98% *R*, 2% *S*) [3]. Recombinant *E. coli* cells harboring the P450 BM-3 gene have already been employed to produce a mixture of 12-, 13-, and 14-hydroxypentadecanoic acid on a preparative scale and with high optical purity [4]. Fine

* Corresponding author. Tel.: +49-711-685-3192; fax: +49-711-685-3196.
E-mail address: itbrsc@po.uni-stuttgart.de (R.D. Schmid).

1381-1177/01/$ – see front matter
PII: S1381-1177(01)00015-7

chemicals with this structure are potential precursors for the synthesis of fragrances or polymer building blocks [4].

The wild-type enzyme exhibits no catalytic activity towards fatty acids with a chain length $<C_{12}$ [1]. The substitution of phenylalanine in position 87 by alanine changed the regioselectivity of the hydroxylation process almost entirely from the subterminal to the terminal position [5]. Terminally or chiral subterminally hydroxylated fatty acids with a chain length $<C_{12}$ would normally constitute interesting novel synthons. Li et al. have therefore, set out to engineer P450 BM-3 for increased catalytic activity towards shorter-chain fatty acids. By combining rational design and directed evolution, they have in fact obtained mutants such as (F87A)LARV, which exhibit greatly enhanced selectivity for shorter-chain ω-(*p*-nitrophenoxy)carboxylic acids (*p*-NCAs) which are fatty acid derivatives [7].

Here we present P450 BM-3 mutants with a selectivity pattern towards these shorter-chain fatty acid derivatives that is even better than that of (F87A)-LARV. They were produced by site-specific randomization mutagenesis at position 87 of the (F87A)LARV mutant as suggested by Li et al. [7]. Fig. 1 shows the evolutionary pathway. In addition, we were able to demonstrate that the use of *p*-NCA pseudosubstrates in the activity assays employing P450 BM-3 mutants can be of high prognostic value for the hydroxylation of free fatty acids by the enzymes. The pseudosubstrate assay can be performed with raw cell extracts and takes only minutes. It therefore, offers the possibility of high-throughput screening for mutants possessing the desired fatty acid specificity. Since only terminal hydroxylations can be monitored with the *p*-NCA assay, we also studied the regioselectivity of the fatty acid conversion products by GLC–MS analysis.

2. Materials and methods

2.1. Materials

All chemicals were of analytical grade or higher quality and were purchased from Fluka (Buchs, Switzerland) or Sigma (Deisenhofen, Germany). Capric and lauric acid were obtained from Henkel (Düsseldorf, Germany), the resins used for the purifications from TosoHaas (Stuttgart, Germany).

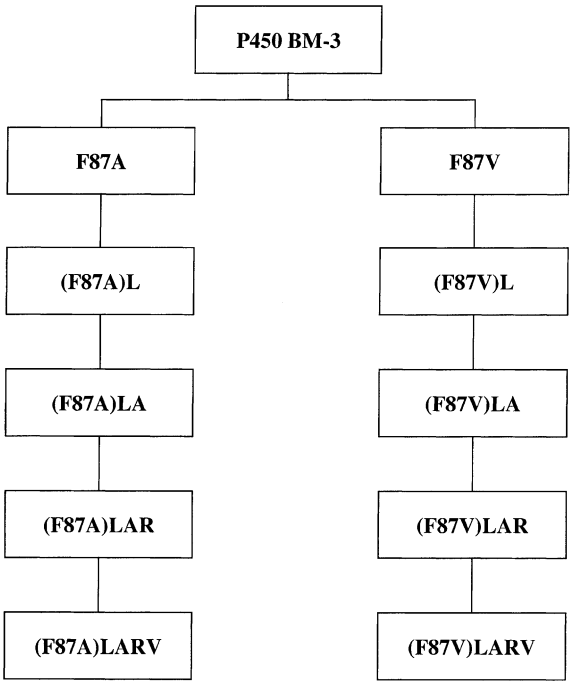

Fig. 1. Evolutionary pathway of P450 BM-3.

2.2. Bacterial strains and mutagenic PCR

The *E. coli* strain DH5α (*sup*E44, *lac*Ul69 (80*lac*Z M15) *hsd*R17 *rec*A1 *end*A1 *gyr*A96 *thi*-1 *rel*A1), obtained from Clontech (Heidelberg, Germany), was used for cloning and protein expression. Isolation and cloning procedures of the P450 BM-3 gene are described elsewhere [6]. The (F87A)LARV variant of P450 BM-3 which contains the five mutations F87A, L188K, A74G, R47F, and V26T is described in Li et al. [7]. The fine-tuning of the (F87A)LARV mutant was carried out by site-specific randomization mutagenesis. The F87V mutant series was created by site-directed mutagenesis of the respective F87A enzyme variants using the Stratagene QuickChange Kit (Stratagene, La Jolla, CA, USA). Primers used for the respective mutations are listed in Table 1. Site-directed mutagenesis involved the exchange of a single codon to replace a certain amino acid. Randomization involved a specific amino acid as in the fine-tuning step and primers with mixed bases (nnn) for the appropriate codon. The reaction conditions involved a 50 μl reaction volume containing 17.5 pmol of each primer,

Table 1
Primers used for PCR

Selected sites/mutations	Primers
F87	5′-gcaggagacgggttgnnnacaagctggacg-3′
Site-specific randomization mutagenesis	5′-cgtccagcttgtnnngaacccgtctcctgc-3′
F87V	5′-gcaggagacgggttggttacaagctggacg-3′
Site-directed mutagenesis	5′-cgtccagcttgtaacgaacccgtctcctgc-3′

20 pmol of template plasmid DNA, 3 U of *Pfu* polymerase, 3.25 nmol of each dNTP. The reaction was started at 95°C (4 min) and thermocycled for 20 cycles: 95°C (1 min), 46°C (2.5 min), 72°C (17 min), and afterwards continued at 72°C (15 min). All PCR product solutions were treated with 20 U *Dpn* I at 37°C for 3 h to digest the initial, non-mutated template DNA prior to the transformation into *E. coli* DH5α cells.

2.3. Enzyme preparation

The enzyme preparation procedure used for the initial round of screening for which only small amounts were required, was performed as described by Li et al. [7]. The large-scale enzyme preparation was carried out using 400 ml terrific broth (TB) medium supplemented with 100 μg/ml ampicillin for plasmid selection. The medium was inoculated with 1 ml of an overnight culture of recombinant *E. coli* DH5α and incubated at 200 rpm and 37°C. At an optical density ($OD_{578\,nm}$) of 0.8–1.0, this medium was used to inoculate 25 l TB medium, also with 100 μg/ml ampicillin, in a 301-fermenter (LP351, Bioengineering, Wald, Switzerland). Fermentation was carried out at 37°C with an aeration of 3.5 l/min, 300 rpm stirrer speed, and an initial pH of 7.5. Prior to inoculation, 2 ml sterile Antifoam O-60 (Sigma–Aldrich, Steinheim, Germany) were added to suppress foam formation. When the $OD_{578\,nm}$ value had reached 0.8–1.0, P450 expression was induced by raising the temperature from 37 to 42°C for 4 h. Native P450 BM-3 and the mutant enzymes were expressed in *E. coli* DH5α; with a yield of 500–700 nmol/l fermenter broth. Cells were harvested by cross-flow filtration over a Filtron (Dreieich, Germany) Centrasette OMEGA (0.3 μm) membrane, supported on a Millipore (Eschborn, Germany) stainless steel holder, and subsequent centrifugation of the concentrated suspension (5000 rpm/10 min). Cells were stored at −20°C until further use.

2.4. Enzyme purification

Up to 15 g (wet weight) DH5α cells were suspended in 20 ml Tris–HCl buffer (25 mM, pH 7.8), thawed on ice, and sonified in an ice bath for 3 min Branson Sonifier W250, Dietzenbach, Germany; output level 80 W, duty cycle 20%). The resulting suspension was centrifuged at 32,500 g for 30 min. Enzymes were purified as described [8] using a BioPilot (Amersham Pharmacia Biotech, Uppsala, Sweden) with a Toyopearl SuperQ 650 column matrix (TosoHaas). For long-term storage, the enzyme solutions were first dialyzed for 4 h in Tris–HCl buffer (25 mM, pH 7.5) to remove residual NaCl from the anion exchange purification step, and then lyophilized with a Lyovac GT2 Lyophilizer (Finn-Aqua, Hürth, Germany). The enzyme lyophilisates showed no loss of activity even after months of storage at −20°C.

2.5. Enzyme activity assay

The activity assay was carried out as described elsewhere [6], except that a Tris–HCl buffer (50 mM, pH 8.0) with KCl (250 mM) was used. Final substrate concentrations varied between 4.5 and 120 μM. Kinetic constants were determined from Lineweaver–Burk plots.

2.6. Enzymatic transformation and product isolation

For the hydroxylation of fatty acids, 20 mg of enzyme lyophilisate (corresponding to a final concentration of 8.5 μM in 20 ml reaction volume) were dissolved in 1 ml reaction buffer (50 mM Tris–HCl, pH 7.8, 250 mM KCl), and incubated for 30 min at 36°C. This solution was added to the reaction buffer (19 ml) containing the fatty acid substrate (3 mM) and 400 μl acetone for solubilization (2% v/v). After a 5 min incubation period [6], enzymatic transformation was started by adding 500 μl NADPH solution

(12.5 mg/ml, 15 mM). NADPH consumption was monitored by measuring the absorption at 340 nm. Stoichiometric conversion requires a total of 4 ml NADPH solution (15 mM); this cofactor was added in 500 μl aliquots, however, to prevent an excessive NADPH concentration that could cause the loss of enzyme activity. Under these conditions, the maximum NADPH concentration determined in the reaction mixture amounted to 0.375 mM. After completion of the reaction, the pH was adjusted to 2.0 by the addition of HCl (5 M) with concomitant precipitation of the fatty acids and their hydroxy derivatives. The slurry was extracted twice with dichloromethane (10 ml each). The organic phases were combined, dried with sodium sulfate, and evaporated. The oily residue was dissolved in dichloromethane (2 ml).

2.7. GLC analysis

N-methyl-*N*-trimethylsiyl-heptafluorobutyramide (MSHFBA, 15 μl) was added to a 10 μl aliquot of the dichloromethane extract solution for derivatization of all hydroxy functions. The mixture was incubated at ambient temperature for 15 min and diluted with dichloromethane (25 μl) prior to GLC and GLC–MS analysis. Gas chromatograms (1 μl samples) were run on a Fisons Mega Series GC (Fisons instruments, Mainz, Germany), equipped with split injector and flameionization detector (FID), and an Optima 5 column (25 m × 0.25 mm, film thickness 0.25 μm; Macherey and Nagel, Düren, Germany). Forepressure was 50 kPa H_2, injector and detector temperature 350°C. Temperature program for capric acid: 100°C (2 min isothermal), 100–140°C (5°/min), 140°C (5 min), 140–300°C (10°/min); for lauric acid: 100°C (2 min), 100–170°C (5°/min), 170°C (5 min), 170–300°C (10°/min); for caprylic acid: 100°C (2 min), 100–300°C (5°/min).

2.8. GLC–MS analysis

GLC–MS spectra of the bis(trimethylsilyl) derivatives were obtained on a Finnigan MAT 95 mass spectrometer (Finnigan MAT, Bremen, Germany), coupled directly to a HP 5890 Series II GC (Hewlett Packard, Waldbronn, Germany); capillary column HP-5 MS (30 m × 0.25 mm, film thickness 0.25 μm); carrier gas 0.065 ml/min He; electron impact ionization (EI) 70 eV.

3. Results and discussion

3.1. Preparation of the (F87V)LARV mutant series

Starting with the enzyme mutant F87A and using the *p*-NCA pseudosubstrate assay [6] it was shown in earlier experiments that enzyme variants with up to five mutations could be obtained which exhibited an altered substrate selectivity and an enhanced preference for 10- and 8-*p*-NCA derivatives. Li et al. [7] obtained the (F87A)LARV mutant through a step-by-step optimization by randomization mutagenesis of the sites 188, 74, 47, and 26 of P450 BM-3. In their experiments, they selected the variant which showed the highest catalytic activity for the 10- and 8-*p*-NCA substrates at each step, i.e. (F87A)L, (F87A)LA, (F87A)LAR, and eventually (F87A)LARV. In particular, site 87 is important for the catalytic activity and substrate specificity of P450 BM-3 [5]. Based on these findings, the 'best' mutant (F87A)LARV obtained by Li et al. was fine-tuned at position 87 by site-specific randomization mutagenesis. Of 100 transformants screened, one mutant was detected that showed a catalytic efficiency of $6.4 \times 10^4\,s^{-1}\,M^{-1}$ towards 8-*p*-NCA. This is approximately twice the catalytic efficiency reported for the (F87A)LARV mutant, i.e. $3.6 \times 10^4\,s^{-1}\,M^{-1}$ [7]. DNA sequencing revealed that Ala87 was substituted to Val in this mutant and the mutant therefore, termed (F87V)LARV.

We now generated the same mutants by site-directed mutagenesis, but all carried the F87V instead of the F87A mutation, i.e. (F87V)L, (F87V)LA, and (F87V)LAR. The catalytic efficiency of these mutants towards the three pseudosubstrates 8-, 10-, and 12-*p*-NCA was determined.

3.2. Catalytic efficiency towards p-NCA pseudosubstrates

The K_M and k_{cat} values, as well as the k_{cat}/K_M ratios of F87V, (F87V)L, (F87V)LA, (F87V)LAR, (F87V)LARV, the wild-type enzyme, and the mutant F87A towards 8-, 10-, and 12-*p*-NCA are given in Table 2. The activities of the wild-type enzyme and

Table 2
Kinetic parameters of P450 BM-3 mutants for hydroxylation of *p*-NCAs with varying chain length[a]

	k_{cat} (s^{-1})			K_M (μM)			k_{cat}/K_M ($s^{-1} M^{-1}$)		
	12	10	8	12	10	8	12	10	8
WT	1.7 ± 0.3	9.7 ± 5.8	–[b]	7.2 ± 2.7	42.0 ± 30.0	–[b]	$2.4 \times 10^5 \pm 4.7 \times 10^4$	$2.3 \times 10^5 \pm 2.7 \times 10^4$	–[b]
F87A	3.5 ± 0.4	5.3 ± 2.5	n.d.[c]	4.4 ± 1.5	59.0 ± 29.0	n.d.[c]	$8.0 \times 10^5 \pm 1.8 \times 10^5$	$9.0 \times 10^5 \pm 1.8 \times 10^3$	n.d.[c]
F87V	0.7 ± 0.1	1.8 ± 0.1	n.d.[c]	3.8 ± 0.8	8.5 ± 1.1	n.d.[c]	$1.8 \times 10^5 \pm 1.5 \times 10^4$	$2.1 \times 10^5 \pm 1.3 \times 10^4$	n.d.[c]
(F87V)L	2.8 ± 0.3	4.7 ± 0.7	n.d.[c]	6.4 ± 1.6	14.2 ± 3.3	n.d.[c]	$4.4 \times 10^5 \pm 6.3 \times 10^4$	$3.3 \times 10^5 \pm 2.8 \times 10^4$	n.d.[c]
(F87V)LA	2.2 ± 0.5	5.9 ± 0.9	4.3 ± 1.3	15.1 ± 4.8	22.7 ± 5.7	197.6 ± 63	$1.5 \times 10^5 \pm 1.3 \times 10^4$	$2.6 \times 10^5 \pm 2.6 \times 10^4$	$2.2 \times 10^4 \pm 3.6 \times 10^2$
(F87V)LAR	1.4 ± 0.1	5.5 ± 1.7	3.9 ± 1.4	8.9 ± 0.8	17.5 ± 4.0	41.4 ± 18	$1.6 \times 10^5 \pm 2.9 \times 10^3$	$3.1 \times 10^5 \pm 2.5 \times 10^4$	$9.4 \times 10^4 \pm 7.1 \times 10^3$
(F87V)LARV	1.4 ± 0.1	7.2 ± 0.8	4.3 ± 2.6	12.3 ± 2.0	44.8 ± 14	67.4 ± 46	$1.1 \times 10^5 \pm 1.0 \times 10^4$	$1.6 \times 10^5 \pm 3.2 \times 10^4$	$6.4 \times 10^4 \pm 5.0 \times 10^3$

[a] pH 8.0, 25°C; as described in Section 2; all measurements were performed twice. 12/10/8: 12-, 10-, 8-*p*-NCA, respectively; WT: wild-type enzyme.
[b] No activity was detected.
[c] No value could be determined since activity was too low to be quantified.

the mutant F87A showed similar values. The catalytic activities of the respective mutants were determined with a pH that was slightly different (8.0 instead of 8.2) than that used in the investigations of Li et al. [7], because a lower pH has positive effects on enzyme activity. The selected pH is always a compromise between protein activity and sensitivity of the assay method; pH values <8.0 usually lead to insufficient *p*-nitrophenolate formation, thus resulting in high measurement errors, especially for slowly converted substrates. To allow for a comparison with the data presented by Li et al. [7], the activities of the wild-type enzyme and the mutant F87A were determined again with the different pH value mentioned above: for F87A, a difference of up to 5% was observed and for the wild-type a catalytic activity that was higher by up to 35% compared with the results of Li et al.

F87A shows the highest activity towards 12-*p*-NCA ($8.0 \times 10^5\ s^{-1}\ M^{-1}$). Its low K_M value (4.4 μM) supports the excellent binding of the 12-*p*-NCA substrate. The k_{cat} value ($3.5\ s^{-1}$) which is the highest of all mutants studied, indicates the best substrate conversion. In the case of 10-*p*-NCA (F87V)L has the best catalytic efficiency, although its K_M (14.2 μM) and k_{cat} ($4.7\ s^{-1}$) values are not optimal. (F87V)LAR, the variant with four mutations, displays the highest activity towards 8-*p*-NCA: the relatively high K_M of 41.4 μM is compensated by a good conversion rate (k_{cat} $3.9\ s^{-1}$). The five-fold mutant (F87V)LARV, however, shows an even better conversion but still less effective substrate binding ability (k_{cat} $4.3\ s^{-1}$, K_M 67.4 μM) than (F87V)LAR.

A comparison of the catalytic activity of the F87A mutant series [7] with that of the F87V mutant series reveals that the pattern of activity changes with each newly inserted mutation is the same even though the absolute values differ, with one exception. While mutant (F87A)LARV shows a higher activity towards 8-*p*-NCA than (F87A)LAR (3.6×10^4 versus $2.3 \times 10^4\ s^{-1}\ M^{-1}$) [7], mutant (F87V)LARV is less active than (F87V)LAR (6.4×10^4 versus $9.4 \times 10^4\ s^{-1}\ M^{-1}$) in the corresponding valine series. Obviously, the amino acid in position 87 is crucial for the orientation of the respective substrate in the binding pocket relative to the catalytic heme center. Oliver et al. have already demonstrated this phenomenon by NMR relaxation studies [5], even though the effect is still not very well-understood in terms of a structure–function relationship.

According to the investigations carried out with pseudosubstrates (8-*p*-NCA), the (F87V)LAR mutant was taken as the most promising candidate as far as hydroxylation ability of short chain substrates is concerned, including for example, capric or caprylic acid, which are not converted by the wild-type enzyme. To transfer the results gained from the assays to natural substrates, it was necessary to determine the conversion pattern towards the natural fatty acid substrates

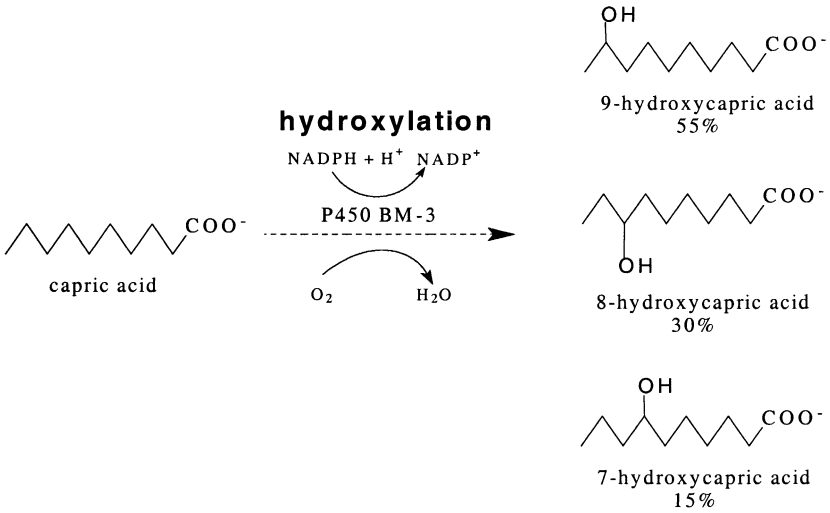

Fig. 2. Reaction scheme of the capric acid hydroxylation.

Table 3
Product ratio and conversion rate for (ω-*n*) hydroxylation of lauric acid catalyzed by the wild-type enzyme (WT) and all F87V mutants[a]

	Conversion rate	Peak 3	Peak 4	Peak 5
Compound		9-Hydroxylauric acid	10-Hydroxylauric acid	11-Hydroxylauric acid
Position		ω-3	ω-2	ω-1
R_t		10.63	11.05	11.32
WT	40	34	28	38
F87V	38	51	25	24
(F87V)L	38	53	30	17
(F87V)LA	39	28	54	18
(F87V)LAR	38	35	50	15
(F87V)LARV	57	34	53	13

[a] Product ratio and conversion rate in % of total substrate; R_t: retention time in min.

Table 4
Product ratio and conversion rate for the hydroxylation of capric acid catalyzed by mutants (F87V)LAR and (F87V)LARV[a]

	Conversion rate	Peak 2	Peak 3	Peak 4
Compound		7-Hydroxycapric acid	8-Hydroxycapric acid	9-Hydroxycapric acid
Position		ω-3	ω-2	ω-1
R_t		11.72	12.47	12.95
(F87V)LAR	38	15	30	55
(F87V)LARV	51	14	33	53

[a] Product ratio and conversion rate in % of total substrate; R_t: retention time in min.

by GLC and GLC–MS. Since the *p*-NCA assay cannot cover subterminal hydroxylations, the GLC–MS analysis also gives an insight into the regioselectivity pattern of each individual enzyme variant.

3.3. Determination of substrate specificity and regioselectivity towards fatty acids

To determine the overall conversion rate and relative regioselectivity of each reaction, a highly reproducible reaction and purification protocol was employed and the reaction products were analyzed with GLC and GLC–MS. Lauric/capric acid and 12-hydroxylauric/10-hydroxycapric acid were used as GLC standards. Fig. 2 shows the typical reaction scheme. The results for lauric acid are given in Table 3, those for capric acid in Table 4; the GLC–MS data are shown in Table 5.

Fig. 3 shows the gas chromatogram of the lauric acid (C12:0) transformation process catalyzed by

Table 5
Structure-relevant fragment ions for the individual enzymatic hydroxylation products of capric and lauric acid (from the GLC–MS of the bis(trimethylsilyl) derivatives)

Capric acid ($x = 8$)			Fragment ion $M^{+\bullet}$[a] (332/360)	Lauric acid ($x = 10$)		
$n = 1$ (ω-1)	$n = 2$ (ω-2)	$n = 3$ (ω-3)		1 (ω-1)	2 (ω-1)	3 (ω-1)
331 ($0_{.9}$)	331 ($0_{.8}$)	331 ($0_{.5}$)	$-H^{\bullet}$[b]	359	359	359
	317 ($27_{.0}$)	317 ($28_{.0}$)	$-(Si-)CH_3{}^{\bullet}$[b]		345	345
317 ($49_{.7}$)				345		
	303 ($100_{.0}$)	289 ($78_{.8}$)	$-CH_3(CH_2)_{n-1}{}^{\bullet}$[b]		331	317
117 ($100_{.7}$)	131 ($83_{.1}$)	145 ($100_{.0}$)	$-(CH_3)SiOCOCH_2(CH_2)_{x-n}$[b]	117	131	145
288 ($40_{.4}$)	274 ($28_{.7}$)	260 ($34_{.1}$)	$\sim(CH_3)_3Si/-CH_3(CH_2)_{n-1}CHO$	316	302	288

[a] $CH_3(CH_2)_{n-1}CH(CH_2)_{x-n}COOSi(CH_3)_3$ with $^{+\bullet}OSi(CH_3)_3$ on the CH carbon ($M^{+\bullet}$).

[b] Straightforward α-fragmentation processes from the molecular ion.

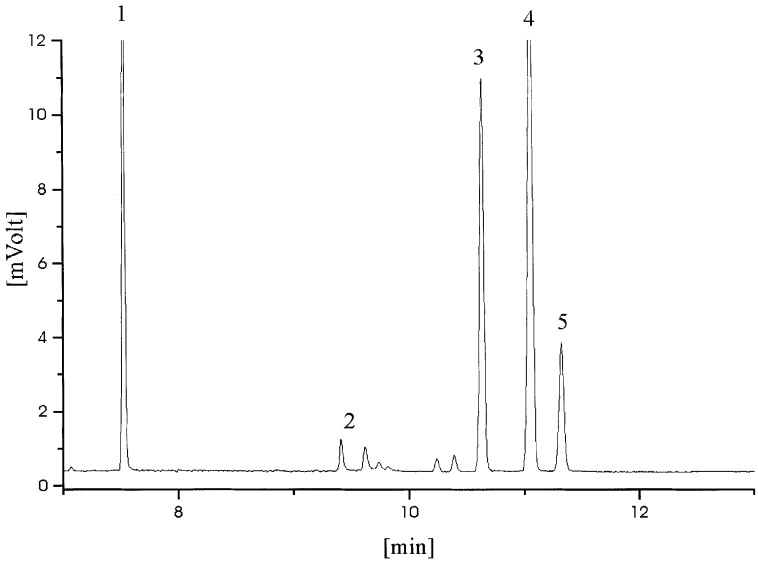

Fig. 3. Gas chromatogram of the educt–product mixture from lauric acid hydroxylation catalyzed by the (F87V)LARV mutant. Peak 1: lauric acid; peak 3: 9-hydroxylauric acid; peak 4: 10-hydroxylauric acid; peak 5: 11-hydroxylauric acid. There is no ω-hydroxylation and only little amounts of ω-4 and ω-5 hydroxylated products (peak 2).

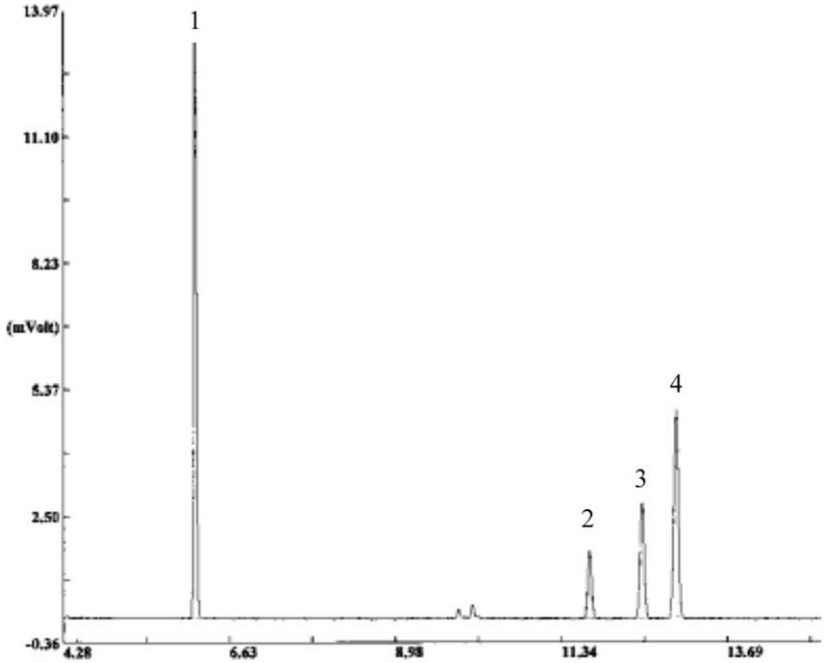

Fig. 4. Gas chromatogram of the educt–product mixture from capric acid hydroxylation catalyzed by (F87V)LARV. Peak 1: capric acid; peak 2: 7-hydroxycapric acid; peak 3: 8-hydroxycapric acid; peak 4: 9-hydroxycapric acid.

the (F87V)LARV mutant revealing regioselectivity. Similar chromatograms were obtained for reactions catalyzed by the other mutants with this substrate. Only the peak areas differed according to the mutant's regioselectivity. The regioselectivity of the purified wild-type enzyme is similar to the results reported by Schneider et al. (ω-3 33%, ω-2 27%, and ω-1 40% [9]), who determined the regioselectivity of P450 BM-3, incorporated in whole cells, towards lauric acid.

The regioselectivity changes with the first mutation, F87V. It leads mainly to the ω-3 hydroxylated product. This position is very important as regards the shift in regioselectivity. When alanine is found at position 87, the fatty acid adopts another conformation in the binding pocket than in the wild-type enzyme. The terminal methyl group is brought closer to the heme and the fatty acid is subsequently hydroxylated in the ω-position [5]. In contrast, the F87V mutant is hydroxylated preferentially in the (ω-3) position. This might be due to an enlargement of the binding pocket caused by the amino acid replacement close to the heme. Thus, the substrate is able to move deeper into the binding pocket, leaving the (ω-3) position closest to the heme where the hydroxylation takes place.

Another change in regioselectivity is observed with the (F87V)LA mutant. In this case, the regioselectivity results mainly in the ω-2 hydroxylated product. The alanine at position 74 is replaced with glycine. This causes a conformational change of the binding pocket in the region of the substrate entrance channel and results in a change of the substrate's position leaving the ω-2 position closest to the heme. The preference for ω-2 hydroxylations is not affected by the subsequent R47F and V26T mutations; (F87V)LAR and (F87V)LARV show nearly the same regioselectivity towards lauric acid as (F87V)LA. In all cases, no terminal hydroxylation occurs.

Fig. 4 shows the gas chromatogram for the capric acid (C10:0) hydroxylation process catalyzed by P450 BM-3 (F87V)LARV. No ω-hydroxylated product could be detected either. Only the (F87V)LAR and (F87V)LARV mutants are able to catalyze the

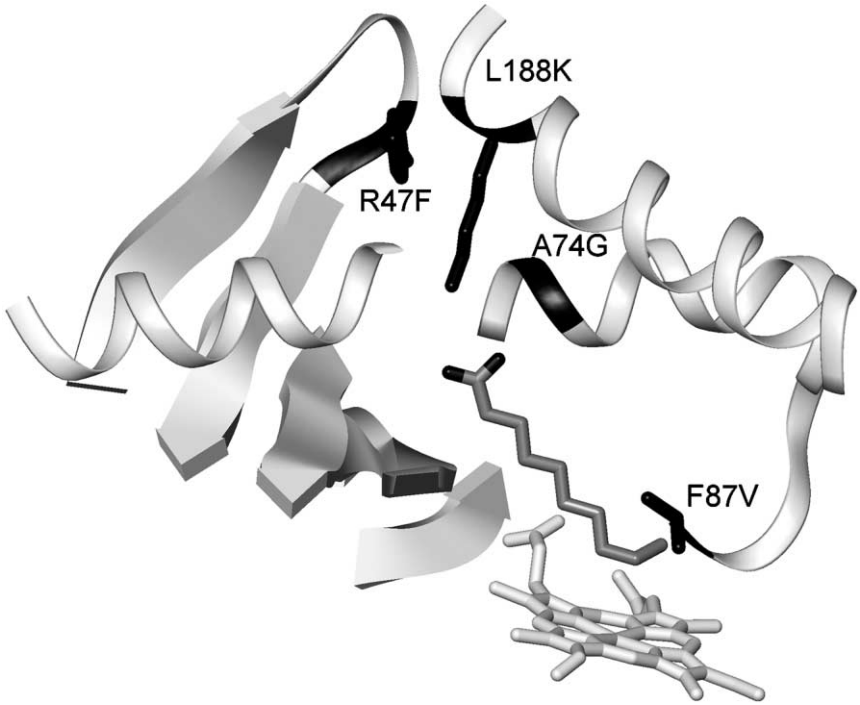

Fig. 5. P450 BM-3 — capric acid complex model for the (F87V)LAR mutant. Mutation sites are shown in black, the substrate in dark grey. The heme center is visible in the lower right corner.

monooxygenation of capric acid. At position 47, arginine represents a carboxylic group binding site that fixates the substrates. In the case of capric acid, the substrate's carbon chain is too short and thus cannot be positioned close enough to the heme to be available for the reaction. The replacement of this binding site in the (F87V)LAR and (F87V)LARV mutants allows the capric acid to come closer to the heme and thus be available for hydroxylation. The regioselectivity of both mutants is nearly identical: the (ω-1) hydroxylation position is preferred. This preference is plausible because the shorter carbon chain of capric compared to lauric acid shifts the (ω-2) and (ω-3) positions too far away from the heme. Another indication for this explanation is that the hydroxylation rate of capric acid catalyzed by (F87V)LARV is twice as high for the (ω-2) position (30%) than for the (ω-3) position (15%). These assumptions are only provisional, however, because they are based on a model created from the X-ray structure of a complex with a much longer substrate [7]. Fig. 5 shows a model of the binding pocket where the capric acid is located inside and the positions of the mutations and the heme domain are indicated. The final mutation in the mutant (F87V)LARV, V26T, does not affect substrate specificity or regioselectivity even though the conversion rates are generally slightly higher than for (F87V)LAR (57/51% versus 38/38%). Kinetic analyses indicate that all three hydroxylation products are formed in the same ratio from the outset; there is no time-dependent preference for any one position in the course of the overall reaction.

All enzyme variants were also tested for their activity towards caprylic acid (C8:0). After the standard work-up process, no conversion products could however, be detected by GLC. This result corresponds to the very low NADPH consumption rate observed after the addition of this substrate. Whether the reaction pocket is too deep or caprylic acid too polar to pass through the narrow hydrophobic entrance channel of the enzyme, is open to speculation.

4. Conclusions

Comparing the behavior of free fatty acids and *p*-NCA derivatives, we could demonstrate some interesting differences between the PM 450 mutants. While all mutants and the wild-type enzyme catalyze the conversion of 10-*p*-NCA, capric acid (C10:0) hydroxylation is catalyzed only by the mutants (F87V)LAR and (F87V)LARV. The 8-*p*-NCA conversion is catalyzed by (F87V)LA, (F87V)LAR and (F87V)LARV, which in turn cannot convert caprylic acid (C8:0). The 8-*p*-NCA is a larger molecule than caprylic acid because the ω-(*p*-nitrophenoxy) moieties of the *p*-NCA substrates are relatively big and require substantial space in the reaction pocket.

The results gained from the fatty acid conversion pattern and the catalytic activity determination led us to conclude that sterically, 8-*p*-NCA might be more similar to capric rather than to caprylic acid, and 10-*p*-NCA more similar to lauric acid (C12:0). These observations would seem to confirm the hypothesis put forward during previous studies carried out by our group [6].

While computer models of the mutants reveal some factors which may indeed contribute to the observed changes in specificity, they must be applied with due caution because no crystal structure of a P450 BM-3 substrate complex is yet available. Relaxation NMR could be an interesting complimentary method to probe for the underlying structure–reactivity relations.

The results obtained with the *p*-NCA assay are sufficiently similar to those obtained from the much more expandable assay with the genuine fatty acid substrates. The *p*-NCA assay can be performed with raw cell extracts and takes only minutes, hence offering high-throughput screening for mutants with the desired fatty acid specificity. Using the pseudosubstrate assay, it was possible to reengineer P450 BM-3 by directed evolution and to identify a mutant, (F87V)LAR, that is also capable of catalyzing the hydroxylation of the natural fatty acid substrate with the desired chain length (Figs. 4 and 5). Thus, ω-*p*-NCA derivatives can serve as pseudosubstrates in lieu of the respective fatty acids with a chain length shorter by two carbon atoms, and allow high-throughput screening in the evolutionary enhancement of P450 BM-3 related enzymes.

Acknowledgements

We thank Markus Fischer for the graphical drawing of the enzyme's active site and the BASF AG for financial support.

References

[1] S.S. Boddupalli, R.W. Estabrook, J.A. Peterson, J. Biol. Chem. 265 (1990) 4233.
[2] I.F. Sevrioukova, H. Li, H. Zhang, J.A. Peterson, T.L. Poulos, Proc. Natl. Acad. Sci. U.S.A. 96 (1999) 1863.
[3] G. Truan, M.R. Komandla, J.R. Falck, J.A. Peterson, Arch. Biochem. Biophys. 366 (1999) 192.
[4] S. Schneider, M.G. Wubbolts, G. Oesterhelt, D. Sanglard, B. Witholt, Biotechnol. Bioeng. 64 (1999) 2833.
[5] C.F. Oliver, S. Modi, M.J. Sutcliffe, W.U. Pimrose, L.Y. Lian, G.C. Roberts, Biochemistry 36 (1997) 1567.
[6] U. Schwaneberg, C. Schmidt-Dannert, J. Schmitt, R.D. Schmid, Anal. Biochem. 269 (1999) 359.
[7] Q.S. Li, U. Schwaneberg, M. Fischer, J. Schmitt, S. Lutz-Wahl, R.D. Schmid, Biochim. Biophys. Acta, submitted for publication.
[8] U. Schwaneberg, A. Sprauer, C. Schmidt-Dannert, R.D. Schmid, J. Chromatogr. A 848 (1999) 149.
[9] S. Schneider, M.G. Wubbolts, D. Sanglard, B. Witholt, Appl. Environ. Microbiol. 64 (1998) 3784.